ALEPH 91-121
PHYSIC 91-108
J. Raab and L. Bauerdick
4.9.1991

Upper Limit on the Tau-Neutrino Mass from $\tau^{\pm} \rightarrow 5\pi^{\pm}(\pi^{\circ})\nu_{\tau}$ Decays

Johannes Raab

Johannes Gutenberg-Universität Mainz

Lothar A. T. Bauerdick

CERN, Div. PPE

Abstract

An upper bound on the tau-neutrino mass has been determined using five-prong tau decays. The data were collected in the 1989 and 1990 LEP runs and correspond to an integrated luminosity of about $8pb^{-1}$. Seven events are observed from which the upper limit $m_{\nu_\tau} < 98\ MeV/c^2$ at 95%CL is extracted.

INTRODUCTION

The best upper limit on the tau neutrino mass m_{ν_τ} is currently set by ARGUS [1] at 35 MeV (95%CL). This limit was obtained by considering the invariant mass of the five pion system in $\tau^\pm \to 5\pi^\pm\nu_\tau$ decays. The five-prong decay is especially suited for a mass bound since the mass of the hadronic system is large relative to the τ lepton mass, $1784.1^{+2.7}_{-3.6}$ MeV; the hadronic mass distribution peaks near $\sim$ 1600 MeV. Previous experiments [1,2,3] have shown that this method improves on bounds obtained from studies of the hadronic energy spectrum in $\tau^\pm \to 3\pi^\pm\nu_\tau$ decays.

In a recent ALEPH note [4] a 77 MeV upper bound on m_{ν_τ} was obtained from a combination of the energy and mass of the hadronic system in the $\tau^\pm \to 3\pi^\pm\pi^\circ\nu_\tau$ mode near the kinematic border. The method presented there is incorrect, or at least incomplete. In the three-prong system considered in [4] the hadronic mass distribution peaks near 1.35 GeV and the energy distribution near $0.75E_{beam}$. The analysis considered only events in a restricted region near the kinematic border. However, in the measurement of m_{ν_τ} it is not allowed to only use events from this limited region. The method in [4] neglects the fact that events from the peak of the kinematic region are found at and beyond the kinematic border because of measurement errors. If the proper likelihood function had been used and all events had been considered, then the upper bound on m_{ν_τ} would have been considerably higher.

This note presents an upper mass limit on m_{ν_τ} from a study of $\tau^\pm \to 5\pi^\pm(\pi^\circ)\nu_\tau$ decays in the 1989 and 1990 runs [5]. Only events in which the other τ decays into a mode with a single charged track are used. The major draw back of the five-prong method comes from the limited statistics since the branching ratios are small, $BR(\tau^- \to 3\pi^-2\pi^+\nu_\tau) = 0.056 \pm 0.016\%$ and $BR(\tau^- \to 3\pi^-2\pi^+\pi^\circ\nu_\tau) = 0.051 \pm 0.022\%$ [6]. With about 8650 $\tau^+\tau^-$ pairs recorded in the 1989 and 1990 runs the expected number of events – excluding all inefficiences – in each five-prong mode is about nine.

The next sections are divided as follows: First, the $\tau^\pm \to 5\pi^\pm(\pi^\circ)\nu_\tau$ event selection is discussed. Second, the method for obtaining the 95%CL upper bound on m_{ν_τ} is presented. This is followed by an estimate of the background and the determination of the mass resolution. In the end the result is given along with some comments.

EVENT SELECTION

The selection of the events in the 1-5 topology proceeds in several steps: All Class 15 events are run through a filter which crudely rejects Bhabhas, $\mu^+\mu^-$-pairs, and multi-hadrons on the basis of calorimeter information only. This is followed by a track selection and a five-prong τ filter. The efficiency of the Class 15 selection for five-

prong decays without and with a π° is estimated from 700 Monte Carlo events to be 0.87 ± 0.02 and 0.81 ± 0.02, respectively. The Monte Carlo uses KORALZ for the $\tau^+\tau^-$ generation and TAUOLA for the subsequent $\tau^\pm$ decays [7]. One τ decay is forced to be in the $\tau^\pm \rightarrow 5\pi^\pm(\pi^\circ)\nu_\tau$ mode, while the other one is decayed according to the known branching ratios.

τ candidate selection: Most of the background is rejected by requiring that

1. There be no energy deposit above 0.2 GeV with $|cos\theta| > 0.96$ in the calorimeters.
2. The number of calorimeter clusters not associated to tracks with energy greater than 0.5 GeV be less than 12 and that their combined energy be less than $\sqrt{s}/2$.
3. The wire energy be greater than $0.03\sqrt{s}$ but less than $0.74\sqrt{s}$.

The first cut is intended to reject events which either have an initial state photon or are not well contained and the second cut partially eliminates low charged multiplicity events containing many neutral particles. The third criterium throws out most Bhabha and μ-pair events. Fig.1 shows the distribution of neutral clusters versus the total neutral energy after the first cut for Monte Carlo $\tau^\pm \rightarrow 5\pi^\pm(\pi^\circ)\nu_\tau$, for Monte Carlo multi-hadrons, and for Class 15 data. Similarly, the wire energy is plotted in fig.2 for Monte Carlo, e^+e^- and $\mu^+\mu^-$ pairs, and data. From the initial sample of 42086 Class 15 events 8487 events pass all three cuts.

track selection: First, all events with pair conversions are removed. All tracks with $P_T > 0.1$ GeV/c, $|cos\theta| < 0.95$, and more than 3 TPC hits are paired with one of opposite charge. The routine QPAIRFD [8] is used to determine the mass and the theta difference of the tracks. The tracks are flagged as a photon conversion if at least one of the tracks has a probability greater than 0.25 of being an electron as given by QFRIPE, their difference of polar angles is less than 0.5° and their invariant mass is less than 40 MeV. In the data 682 events are rejected.

In the remaining analysis only tracks with more than 4 TPC hits, $|z0| < 10$ cm, $|d0| < 3.5$ cm, $P_T > 0.5$ GeV/c, and $|cos\theta| < 0.95$ are considered. No tracks are allowed to fail these cuts and exactly six tracks must satisfy these criteria, otherwise the event is rejected. Finally, the total track energy of the six tracks must exceed $0.25\sqrt{s}$. The distributions of good and bad tracks and of the total momentum for Monte Carlo and data are shown in fig.3. The slight enhancement in the Monte Carlo at eight good tracks is due to three-prong decays on the other side. The requirement of exactly six tracks gives about a 50% loss of efficiency. A scan of the Monte Carlo events shows that in most five track events a track was lost due to an overlap with another track

resulting either in unresolved TPC coordinates and/or in a false track fit. At this stage 122 $\tau^{\pm} \rightarrow 5\pi^{\pm}(\pi^{\circ})\nu_{\tau}$ candidates remain.

five-prong τ candidate selection: The selection of the $\tau^{+}\tau^{-}$ pair decays with the one-five topology proceeds as follows: The event is divided into two hemisperes using the plane through the interaction point with normal vector along the charged particle thrust direction. The track multiplicities in the two hemisperes must be compatible with the 1-5 topology criterium. The total charge in the two hemispheres must be of opposite sign. The momentum of every track on the five-prong side must be between 0.5 GeV/c and 34 GeV/c and the maximum opening angle between any pair of tracks must be less than 15°. In order to assure containment and well measured tracks the 1-prong jet must have $|cos\theta| < 0.87$ relative to the beam direction. In addition, the acollinearity angle between the two jets is required to be less than 14°. Some of these variables are shown in fig.4. Only 12 events pass the cuts.

background rejection: To ensure that the events are free from conversions none of the five tracks are allowed to be compatible with electrons. The standard cuts on transverse and longitudinal shower development are used, $R_T > -3.$ and $-2.4 < R_L < 3.0$. The distribution of the electromagnetic shower estimators are shown in fig.5 for Monte Carlo and data. Two events contain an electron and are rejected.

π° reconstruction: In order to reconstruct π°s the region within the cone of half angle 30° (twice the allowed opening angle between tracks) centered on the five-prong jet axis is searched for neutral clusters [9]. When there are two or more clusters then they are combined in pairs, the invariant mass computed, and classified as a π° if the reconstructed mass is within ± 70 MeV of the nominal π° mass and the energy is greater than 2 GeV. These clusters are also classified as a π° if their energy is greater than 2 GeV. Similarly, if a single neutral cluster above 1 GeV is found, it is deemed a π°. Fig.6 shows the π° energy distribution for Monte Carlo events. Events with neutral clusters which did not qualify as π°'s are rejected. One event is removed.

vertex requirement and track refit: The five tracks are then refit with the constraint of a common vertex [10]. Each track must have a probability of greater than 10^{-16} of belonging to the vertex and the probability that all five tracks are from the same vertex must exceed 10^{-16}. The smallest track probabilty versus the vertex probability is shown in fig.7. Two events fail this cut. At this point seven five-prong candidates remain, of which one contains a π°.

Finally we compute the invariant mass of the five-prong system assuming that all tracks are pions. The error on the mass is calculated with the full covariance matrix for

each track and a diagonal matrix for the π^0. Particle-particle correlations are assumed to be negligible. The resulting mass spectrum of the τ candidates is given in fig.8. The events are also listed in Table 1.

METHOD TO OBTAIN THE 95%CL MASS LIMIT

The 95% CL limit on m_{ν_τ} is determined with a likelihood function which gives the probability density for obtaining the observed mass distribution. It is necessary to weight every observed event with the matrix element and the corresponding phase space. For the purely charged five-prong τ decay this function contains the following pieces:

1. The weak hadronic matrix element, which describes the transition $\tau^- \rightarrow h^-\nu_\tau$, where h^- is a hadron of spin 1 or 0 which subsequently decays.
2. The phase space factor for this two–body system.
3. The matrix element which describes the decay of the hadron into 5 pions. In this note we assume that there is no resonance structure in the decay, e.g., the matrix element is constant with M_h.
4. The five-body phase space $\Phi(M_h, m_\pi)$ for the hadronic decay.
5. The mass resolution R assumed to be Gaussian, and the efficiency ϵ taken as a linear function of M_h.

The first two items can be computed analytically, while the 5-body phase space must be generated, tabulated and/or parameterised. It should be noted that the neutrino mass appears only in the first two items, and that the hadronic decay is a purely multiplicative factor which is complicated if resonances are included.

For the case that the hadron has spin 1 one calculates for the first two terms [3,11]

$$\frac{d\Gamma^c}{dM_h^2} \propto \frac{M_h^2}{m_\tau^2 M_h^2}\Big((m_\tau^2 - M_h^2)(m_\tau^2 + 2M_h^2) - m_\nu^2(2m_\tau^2 - M_h^2 - m_\nu^2)\Big) \times \sqrt{(m_\tau^2 - M_h^2)^2 - m_\nu^2(2m_\tau^2 + 2M_h^2 - m_\nu^2)},\Phi(M_h, m_\pi)$$

When the final state contains a π^0 the shape of the mass spectrum is obtained with the help of CVC and e^+e^- experiments. CVC relates the vector part of the weak charged current to the isovector part of the electromagnetic current. Inclusive the phase space factor, it is found that [11]

$$\frac{d\Gamma^0}{dM_h^2} \propto \frac{\sigma^{(1)}_{e^+e^-}(M_h^2)}{\sigma_{pt}(M_h^2)}\Big((m_\tau^2 - M_h^2)(m_\tau^2 + 2M_h^2) - m_\nu^2(2m_\tau^2 - M_h^2 - m_\nu^2)\Big) \times \sqrt{(m_\tau^2 - M_h^2)^2 - m_\nu^2(2m_\tau^2 + 2M_h^2 - m_\nu^2)},$$

with $\sigma_{pt}(s) = \frac{4\pi\alpha}{3s}$ the e^+e^- annihilation cross section into $\mu^+\mu^-$, and $\sigma^{(1)}_{e^+e^-}(s)$ the experimental cross section for $e^+e^- \to 6\pi$ [12]. In this note $\sigma^{(1)}_{e^+e^-}(s)$ is parametrised as a linear function in M_h. The Monte Carlo mass spectra for $m_\nu = 0$ MeV of the two modes are shown in fig.9. The curves are given by the above equations for $\frac{d\Gamma}{dM}$.

On folding this with the experimental resolution function

$$\mathcal{R}(M_h, \sigma_h) = \frac{1}{\sqrt{2\pi}\sigma_h} \; e^{-\frac{(M-M_h)^2}{2\sigma_h^2}},$$

the 5-body phase space, and an efficiency function $\epsilon^c(M_h)$ the probability density for observing event i with hadronic mass M_i and resolution σ_i is obtained. As a function of the neutrino and hadron mass, one finds for the $\tau^\pm \to 5\pi^\pm\nu_\tau$ mode

$$P_i^c(m_\nu, M_i) = \frac{\int_{5m_\pi}^{m_\tau - m_\nu} \frac{d\Gamma^c}{dM}(M, m_\nu)\mathcal{R}(M - M_i, \sigma_i)\epsilon^c(M)dM}{\int_{5m_\pi}^{m_\tau - m_\nu} \frac{d\Gamma^c}{dM}(M, m_\nu)\epsilon^c(M)dM}.$$

Similarly, for the $\tau^\pm \to 5\pi^\pm\pi^\circ\nu_\tau$ channel the probabilty function is

$$P_i^\circ(m_\nu, M_i) = \frac{\int_{5m_\pi + m_{\pi^\circ}}^{m_\tau - m_\nu} \frac{d\Gamma^\circ}{dM}(M, m_\nu)\mathcal{R}(M - M_i, \sigma_i)\epsilon^\circ(M)dM}{\int_{5m_\pi + m_{\pi^\circ}}^{m_\tau - m_\nu} \frac{d\Gamma^\circ}{dM}(M, m_\nu)\epsilon^\circ(M)dM}$$

The likelihood function, i.e., the combined probability density of obtaining the observed hadronic mass distribution is then

$$\mathcal{L}(m_\nu) = \prod_{i,j} P_i^j(m_\nu, M_i),$$

where j labels the two decay modes. The 95%CL upper bound on the neutrino mass, $m_\nu(95)$, is determined from the condition that

$$0.95 = \frac{\int_0^{m_\nu(95)} \mathcal{L}(m_\nu)dm_\nu}{\int_0^\infty \mathcal{L}(m_\nu)dm_\nu}.$$

Alternatively, one could define the 95%CL as that point at which the likelihood function has fallen to $e^{-1.96}$ of its maximum value.

However, in using the above probability density great care must have been taken to select true five-prong events and/or to have estimated the backgrounds and mass resolution properly. Consider the observed event at 1975 ± 79 MeV. The mass and resolution

are still compatible with a five-prong τ decay, although with a small probability. If the mass resolution is correct and the event is incomptible with background, then this event pushes the mass bound to a low value.

On the other hand, incompletely reconstructed $\tau \rightarrow 5\pi^{\pm}\pi^{\circ}$ or mis-identified three-prong decays with a conversion have the opposite effect. The reconstructed hadronic mass is too small which leads to a large ν-mass.

Thus, it is very important to understand the events, to ascertain their true resolution, and to verify that they are not background.

BACKGROUND

The multi-hadronic backround was studied using an equivalent set of 600k multi-hadronic Monte Carlo Z° decays[2]. The events were preselected at the generator level. All events with less than 8 tracks were retained. The surviving 3017 events were fully simulated and reconstructed. Only 757 remained after the standard Class 15 filter. In the end, no events survived the selection. Most were rejected by the crude multi-hadron rejection (see fig.1), and none passed the above τ selection criteria. Thus the multi-hadronic background is taken to be less than 0.3 events and will be neglected.

To estimate the background from three-prong decays with a conversion an equivalent set of 30k τ-pairs in the $\pi^{-}\pi^{+}\pi^{\pm}(\pi^{\circ})$ modes was generated. The three-prong mode, with and without neutrals, could be a very large background source because for every five-prong decay there are more than 100 three-prong τ decays. The events were sent through the Galeph/Geant tracking and rejected unless the charged particle multiplicity increased by at least two. The retained events underwent the complete simulation and reconstruction. No events survived all the cuts. This leads to a negligible background of less than 0.29 events.

Finally, the contribution of incompletely or falsely reconstructed π°'s was determined. To this end, 381 $\tau^{\pm} \rightarrow 5\pi^{\pm}\pi^{\circ}\nu_{\tau}$ and 319 $\tau^{\pm} \rightarrow 5\pi^{\pm}\nu_{\tau}$ decays with $m_{\nu} = 0$ were generated and fully simulated. After the Class 15 selection, respectively, 308 and 279 decays remain. After all cuts, 56 are correctly identified as $\tau^{\pm} \rightarrow 5\pi^{\pm}\nu_{\tau}$ and 7 falsely, 61 correctly as $\tau^{\pm} \rightarrow 5\pi^{\pm}\pi^{\circ}\nu_{\tau}$ and none incorrectly. The final efficiencies including the Class 15 selection as a function of the hadron mass are shown in fig.10.

The misidentified $\tau^{\pm} \rightarrow 5\pi^{\pm}\pi^{\circ}\nu_{\tau}$ as $\tau^{\pm} \rightarrow 5\pi^{\pm}\nu_{\tau}$ decays demands a slight modification to the above probability distribution for the $\tau^{\pm} \rightarrow 5\pi^{\pm}\nu_{\tau}$ mode. The non-observance of the π° should be accounted for. The probabilty of reconstructing a charged

[2] It is assumed that LUND correctly describes very low multiplicity hadronic events.

five-prong becomes

$$P_i(m_\nu, M_i) = \kappa P_i^c(m_\nu, M_i) + (1-\kappa)P_i^f(m_\nu, M_i),$$

where $\kappa = 0.9$ is the relative fraction of correctly reconstructed events, and $P_i^f(m_\nu, M_i)$ gives the probability that a given M_i is from the $\tau^\pm \to 5\pi^\pm\pi^\circ\nu_\tau$ distribution. Both, κ and P_i^f are determined from Monte Carlo. P_i^f is obtained by shifting the $5\pi^\pm$ mass spectrum for $\tau^\pm \to 5\pi^\pm\pi^\circ\nu_\tau$ decays obtained for $m_\nu = 0$ MeV down by m_ν (This is not quite correct but Monte Carlo events for different m_ν were not generated. The chosen procedure introduces very little bias since κ is close to unity.). The spectrum of the misidentified events is shown in fig.11.

MASS RESOLUTION

The mass resolution as computed with the standard error matrices is usually too optimistic and should be scaled up by some factor. In addition, it is important to verify the assumption of Gaussian errors. The resolution and the scale factor are a **property of the given event** and must be determined on an event by event basis. To obtain the resolution for the $\tau^\pm \to 5\pi^\pm\nu_\tau$ candidates each one is passed through Galeph one to two hundred times and re–reconstructed. The idea of the method is to find the intrinsic detector resolution which is determined by multiple scattering, the gas ionization, *etc.*. The single event resolution does not properly account for fluctuations in these quantities. The width of the distribution of the mass estimator $(m_{true} - m_{rcn})/\sigma$ determines the scale factor. These distributions for the candidates are shown in fig.12.

A similar scheme for reprocessing and re-reconstructing the π° in the $\tau^\pm \to 5\pi^\pm\pi^\circ\nu_\tau$ event was not implemented. Instead the contribution of the π° to the resolution was estimated from the Monte Carlo. The last plot in fig.12 shows the ratio $(m_{rcn} - m_{true})/\sigma_{rcn}$ for all $\tau^\pm \to 5\pi^\pm\pi^\circ\nu_\tau$ MC events. A multiplicative scale factor is applied in addition to the one obtained for the charged mass. Table 1 gives a summary of the events and their final masses with associated errors.

RESULTS

The probability densities of the seven $\tau^\pm \to 5\pi^\pm\nu_\tau$ events are plotted in fig.13. Each one is normalized to unit area. The last plot in the figure is a cutout from the integrated likelihood as a function of m_ν, i.e., the vertical axis is the confidence level. Thus, reading from the last plot:

$$m_{\nu_\tau} < 98 \quad \text{MeV} \qquad (95\%\text{CL}).$$

Fig.14 shows the data points superimposed on the expected distribution for $m_{\nu_\tau} = 0$ and 98 MeV.

Table 1 *Summary of* $\tau^{\pm} \to 5\pi^{\pm}(\pi^{\circ})\nu_{\tau}$ *candidates.*

Candidate	Run	Event	mass (GeV/c^2)	error (GeV/c^2)	scale factor	final error (GeV/c^2)
$\tau^{\pm} \to 5\pi^{\pm}\nu_{\tau}$						
1	5158	4656	1.3375	0.0105	3.4	0.036
2	5166	1984	1.6363	0.0089	1.1	0.010
4	7252	4616	1.4954	0.0083	1.73	0.014
4	8489	4451	1.4928	0.0095	1.85	0.018
5	7418	701	1.4518	0.0156	1.14	0.018
6	7849	7984	1.9759	0.0795	1.59	0.126
$\tau^{\pm} \to 5\pi^{\pm}\pi^{\circ}\nu_{\tau}$						
7	8331	6971	1.7535	0.0404	1.24×1.1	.055

The data sample corresponds to about 8650 τ pair events. The combined $\tau^{\pm} \to 5\pi^{\pm}(\pi^{\circ})\nu_{\tau}$ efficiency is $17.8 \pm 1.5\%$. The total five-prong branching ratio is then

$$BR(\tau^{\pm} \to 5\pi^{\pm}(\pi^{\circ})\nu_{\tau}) = 0.0022 \pm 0.0008\ (stat).$$

This agrees fairly well with the recent ALEPH result on the topological branching ratios [11].

CRITIQUE, DISCUSSION, AND IMPROVEMENTS

The track and π° reconstruction could be improved. Perhaps a detailed analysis of the TPC pulse shapes will help in separating close tracks. The π° efficiency can probably be raised through a more detailed cluster and shower profile analysis. This should also reduce the misidentification of $\tau^{\pm} \to 5\pi^{\pm}\pi^{\circ}\nu_{\tau}$ as $\tau^{\pm} \to 5\pi^{\pm}\nu_{\tau}$ decays. An improvement in resolution is needed only insofar the long tails are brought under control. A single mismeasured event can produce a wrong estimate of m_{ν}. In addition, the π° definition can shuffle events between the two decay modes. In part this is taken care of by the modified probability function which must rely on the Monte Carlo.

Clearly, more Monte Carlo for the background studies is needed. At 95%CL one should have counted one background event from the multi-hadron study and one from the 3-prong study.

Finally, the major improvement in the mass limit should come from higher statistics. This increases the chance of getting an event near the τ mass. Unfortunately, one cannot say exactly how many events are needed for a 10 MeV bound. A bit of luck is involved

there. To compare with ARGUS which has about 20 good events for the 35 MeV upper limit, one would need the canonical 10^6 Z° events.

REFERENCES

[1] ARGUS Collaboration, Phys. Lett. B 202 (1988), 149.

[2] ARGUS Collaboration, Phys. Lett. B 163 (1985), 404.

[3] HRS Collaboration, Phys. Rev. Lett. 56 (1986), 1039; MARKII Collaboration, Phys. Rev. Lett. 54 (1985), 2489.

[4] U. Stiegler, ALEPH note, June 1991.

[5] See also the transparencies from the ALEPH internal meeting on τ neutrino mass measurements, 26.11.1990, edited by L. Bauerdick.

[6] Particle Data Group, (1990).

[7] KORALZ, S. Jadach, B.F.L. Ward and Z. Was, CERN preprint TH-5994/91; TAUOLA, S. Jadach, J. Kühn and Z. Was, Comp. Phys. Comm. 64 (1991), 275.

[8] D. Cinabro, routine QPAIRFD.

[9] L. Bauerdick, FV package.

[10] A. Rougé, routine CLUSTENE.

[11] F. Gilman and D. Miller, Phys. Rev. D 17, (1977), 1846.

[12] G. Cosme *et al.*, Nucl. Phys. B 152 (1979), 215; more precise results from DM2 should be forthcoming.

[13] M. Davier and Z. Zhang, ALEPH note, July 1991.

FIGURES

Fig.1 Number of neutral calorimeter clusters above 0.5 GeV versus total neutral energy for $\tau^{\pm} \rightarrow 5\pi^{\pm}(\pi^{\circ})\nu_{\tau}$ Monte Carlo, low multiplicity hadronic Z° decays generated with JETSET7.3, and Class 15 data.

Fig.2 Wire energy distribution for $\tau^{\pm} \rightarrow 5\pi^{\pm}(\pi^{\circ})\nu_{\tau}$ MC, $e^{+}e^{-}$ and $\mu^{+}\mu^{-}$ pairs, and data.

Fig.3 Distribution of the number of "good" and "bad" tracks, and the total momentum of the six selected tracks.

Fig.4 Top: Plot of the maximum track momentum in the five-prong jet. Middle: The distribution of the maximum angle between the tracks in the five-prong jet. Bottom: The acollinearity angle distribution.

Fig.5 Transverse versus longitudinal ECAL shower estimators;

Fig.6 Top: energy distribution of single neutral clusters. Middle top to bottom: Mass of π° versus π° energy and the projections.

Fig.7 Scatter plot of $-\log prob$ of the "worst track" versus that of the vertex (events with $-logprob = 21$ are overflow).

Fig.8 Hadronic mass distribution and associated uncorrected errors of $\tau^{\pm} \rightarrow 5\pi^{\pm}\nu_{\tau}$ and $\tau^{\pm} \rightarrow 5\pi^{\pm}\pi^{\circ}\nu_{\tau}$ candidates.

Fig.9 Hadronic mass distribution for $\tau^{\pm} \rightarrow 5\pi^{\pm}(\pi^{\circ})\nu_{\tau}$ decays from KORALZ superimposed on the functions used in the 95% CL determination.

Fig.10 Detection efficiency versus hadronic mass.

Fig.11 Mass obtained from the five tracks in all $\tau^{\pm} \rightarrow 5\pi^{\pm}\pi^{\circ}\nu_{\tau}$ events. The hashed area indicates the seven falsely identified events.

Fig.12 The resolution functions for the candidate events. The bottom row corresponds to the π° candidate.

Fig.13 The probabilty distributions as a function of the neutrino mass in GeV for each candidate event; bottom middle: combined probability of all events; bottom right: the neutrino mass versus the confidence level (note the suppressed zero on the vertical axis).

Fig.14 Hadronic mass distributions with corrected errors superimposed on the calculated distributions for $m_{\nu} = 0$ MeV (solid) and $m_{\nu} = 98$ MeV (dashed).

Fig. 1

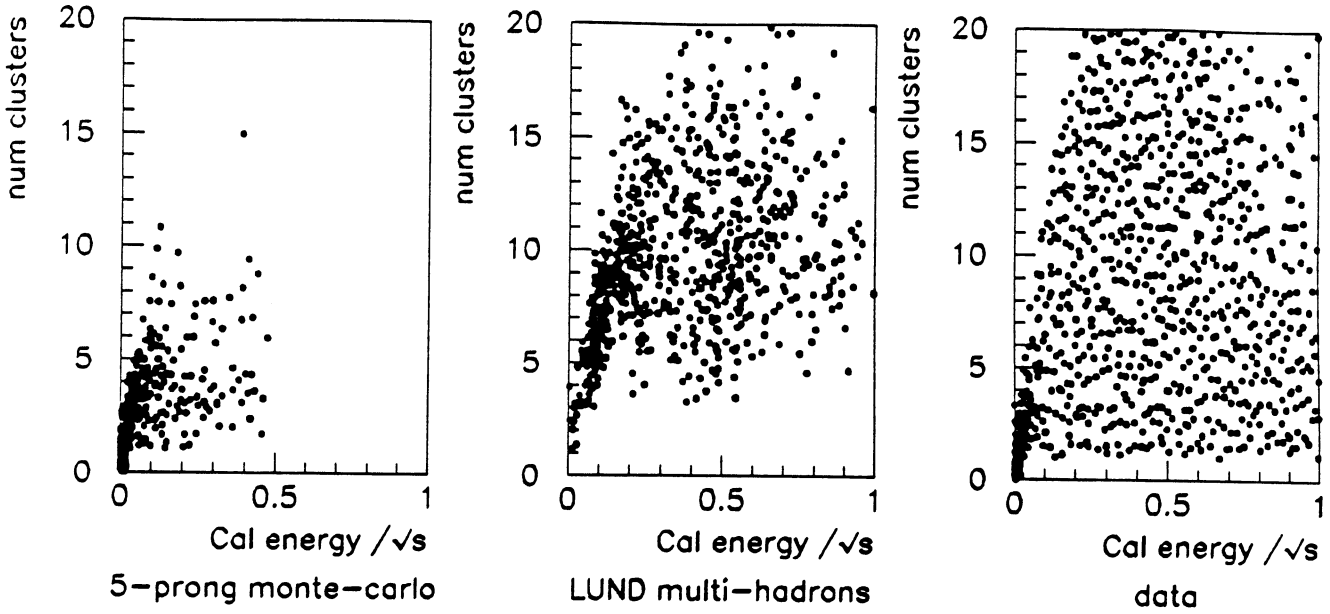
num clusters
20
15
10
5
0
0
0.5
1
Cal energy /√s
5−prong monte−carlo
num clusters
20
15
10
5
0
0
0.5
1
Cal energy /√s
LUND multi−hadrons
num clusters
20
15
10
5
0
0
0.5
1
Cal energy /√s
data

Fig. 2

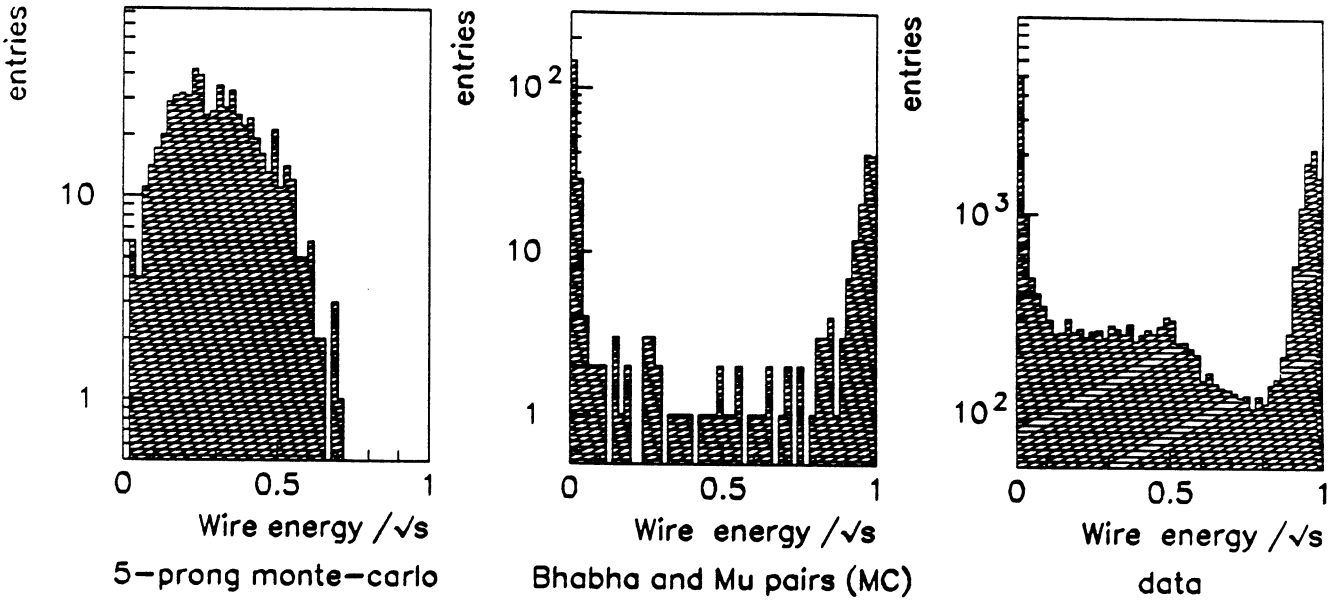
entries
10
1
0
0.5
1
Wire energy /√s
5−prong monte−carlo
entries
10²
10
1
0
0.5
1
Wire energy /√s
Bhabha and Mu pairs (MC)
entries
10³
10²
0
0.5
1
Wire energy /√s
data

Fig. 3

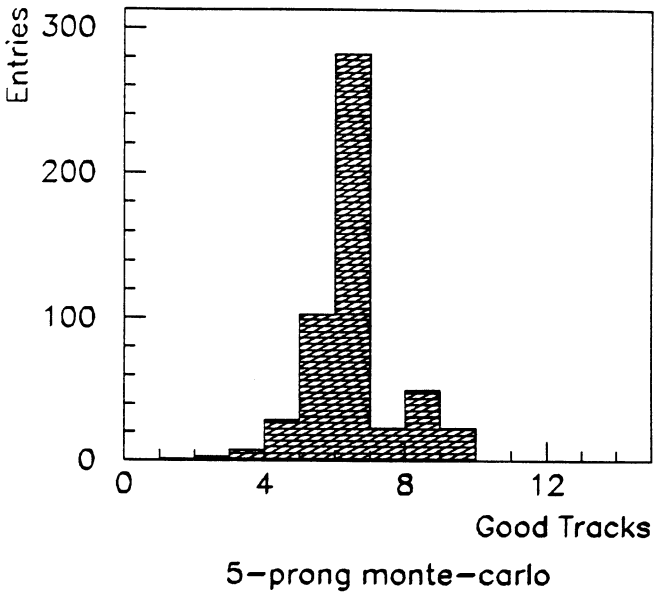

5-prong monte-carlo

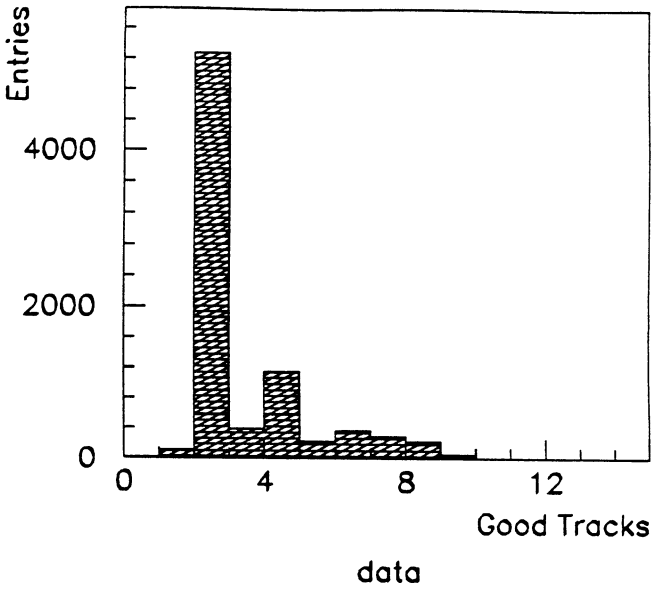

data

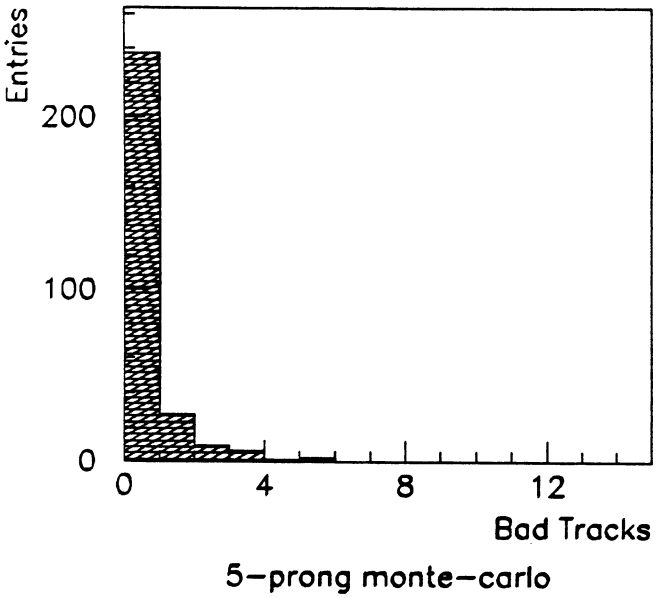

5-prong monte-carlo

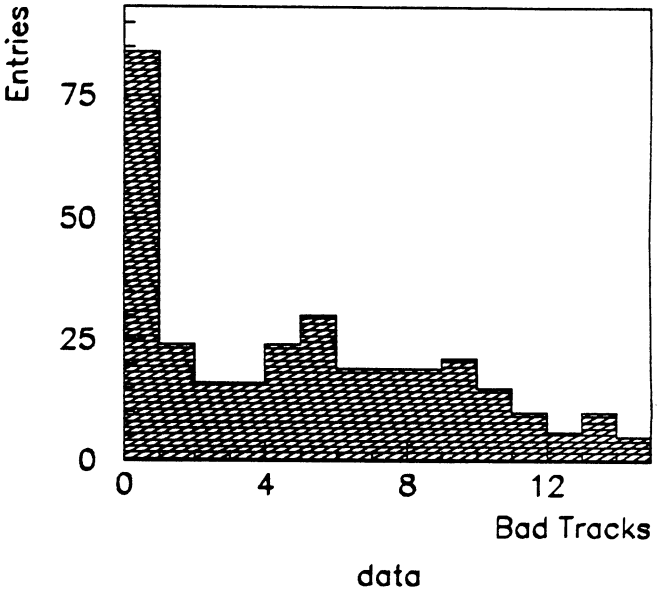

data

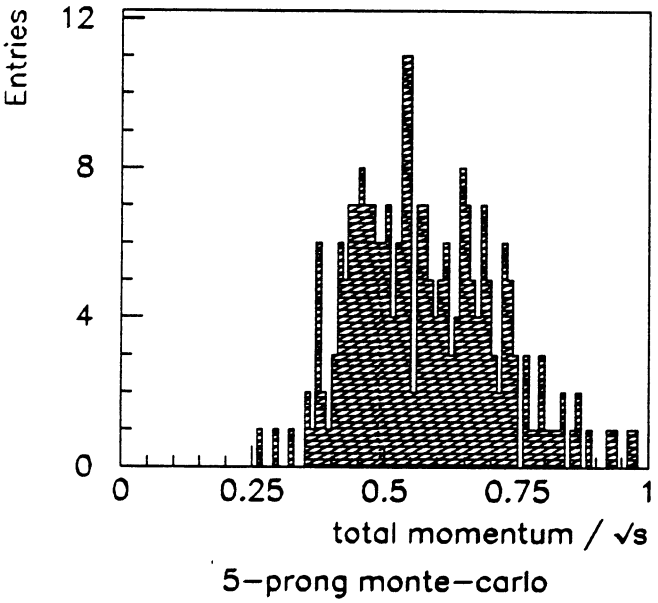

5-prong monte-carlo

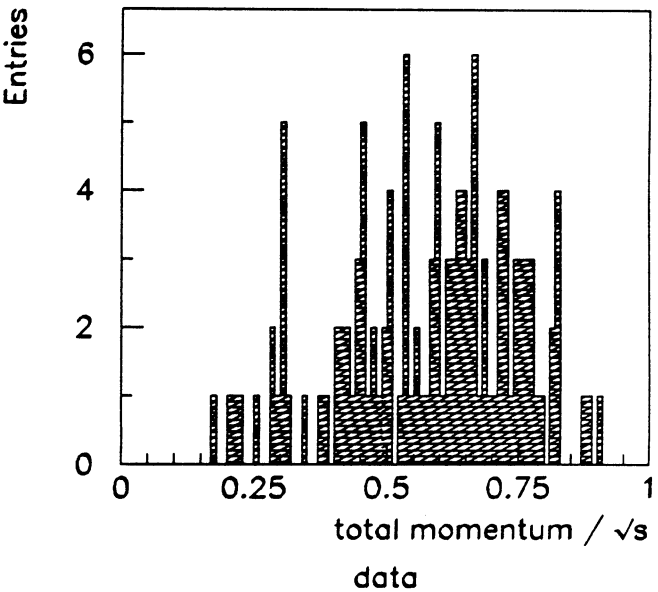

data

Fig. 4

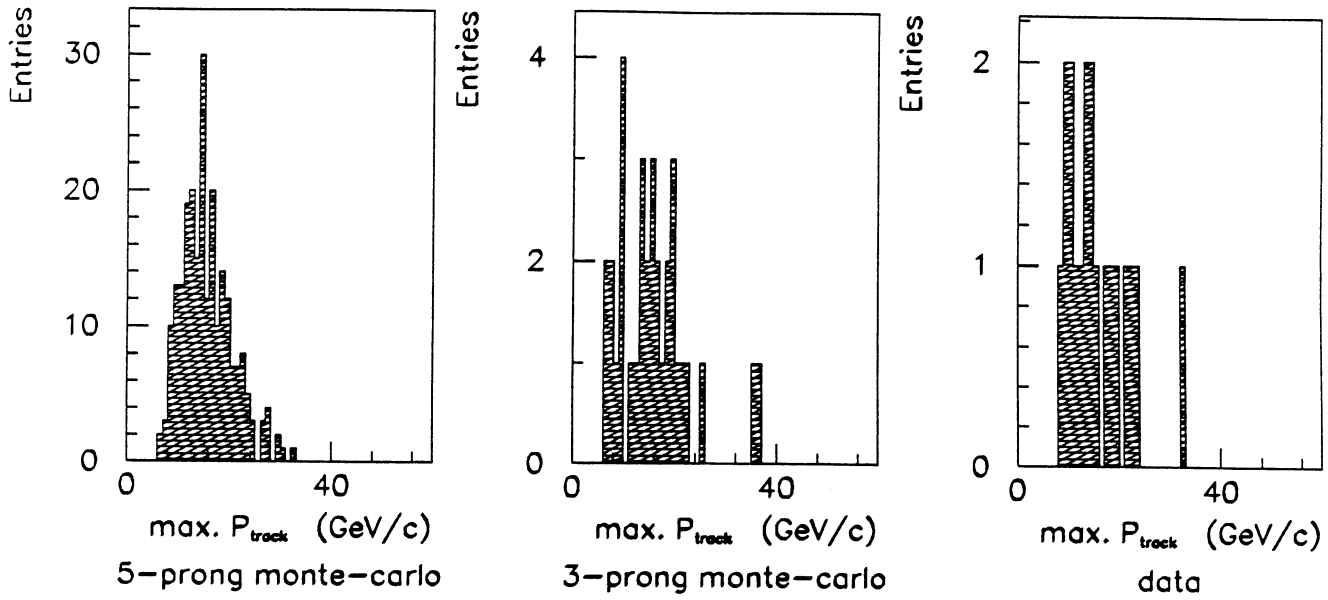
Entries
30
20
10
0
0
40
max. P_{track} (GeV/c)
5-prong monte-carlo
Entries
4
2
0
0
40
max. P_{track} (GeV/c)
3-prong monte-carlo
Entries
2
1
0
0
40
max. P_{track} (GeV/c)
data

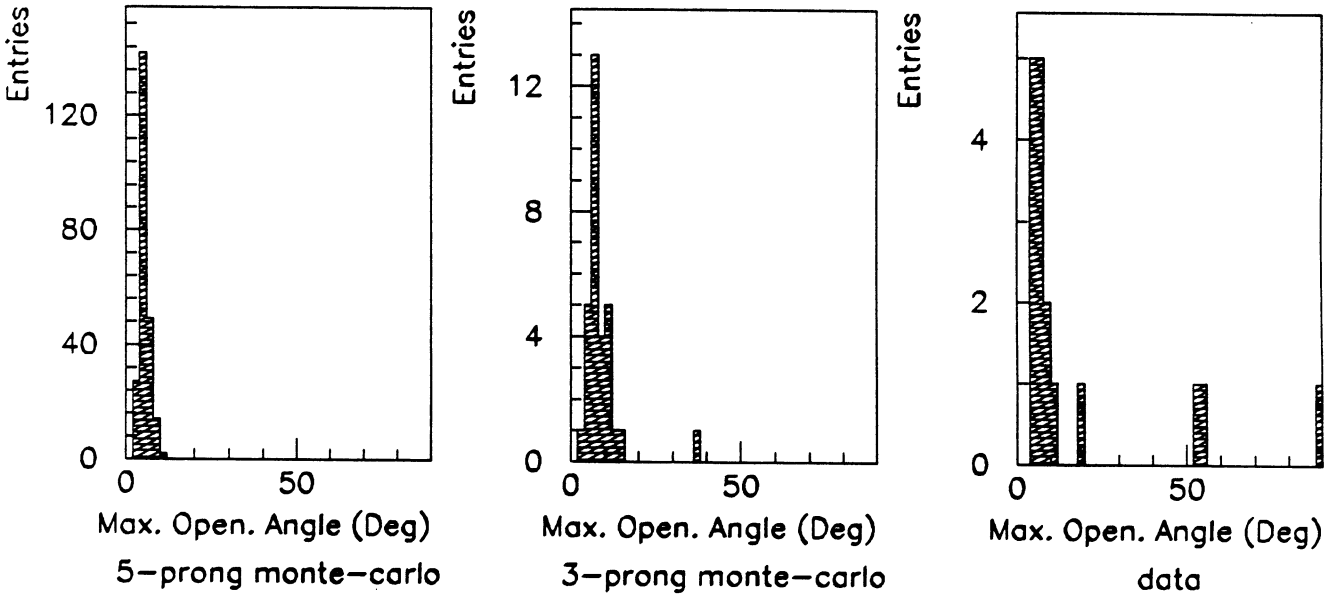
Entries
120
80
40
0
0
50
Max. Open. Angle (Deg)
5-prong monte-carlo
Entries
12
8
4
0
0
50
Max. Open. Angle (Deg)
3-prong monte-carlo
Entries
4
2
0
0
50
Max. Open. Angle (Deg)
data

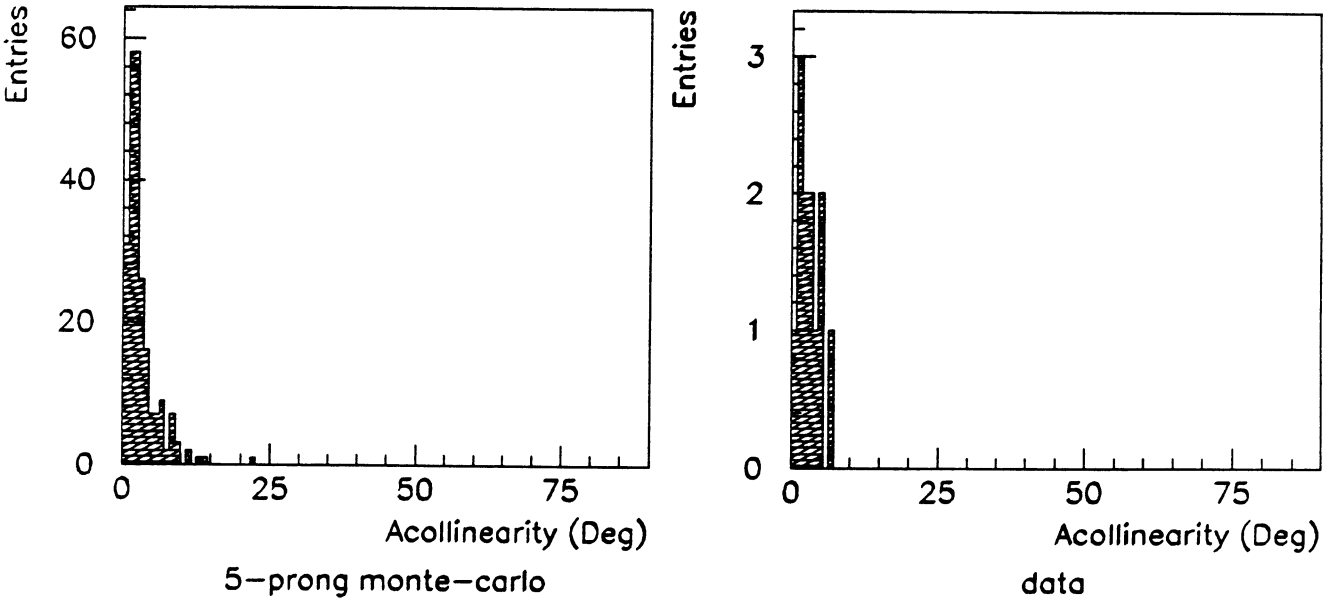
Entries
60
40
20
0
0
25
50
75
Acollinearity (Deg)
5-prong monte-carlo
Entries
3
2
1
0
0
25
50
75
Acollinearity (Deg)
data

Fig. 5

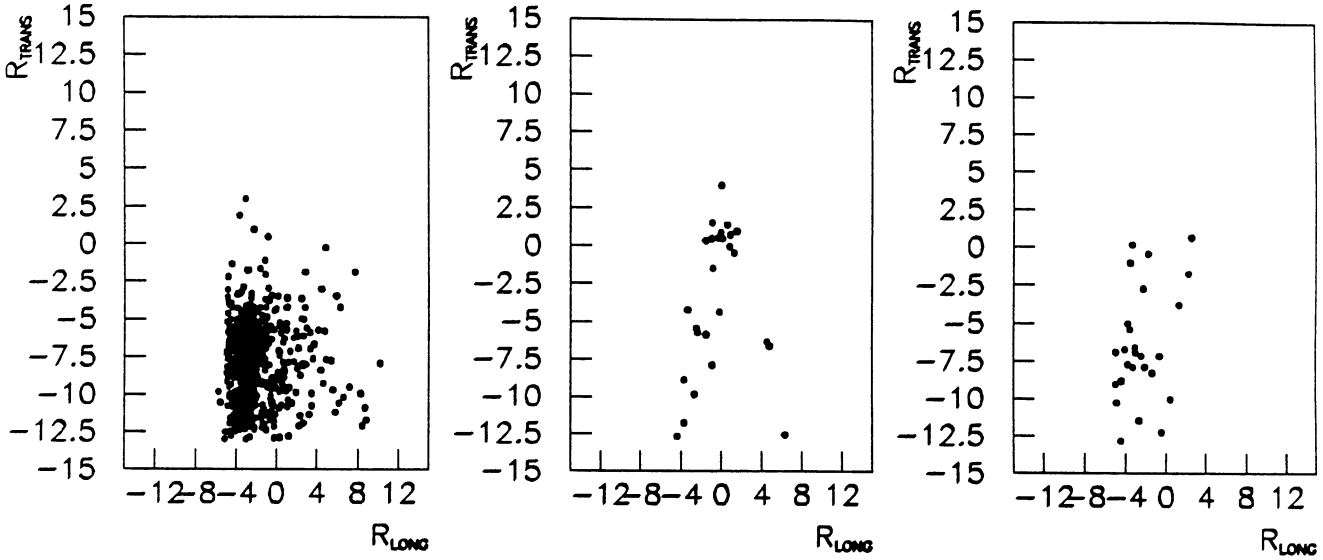

5−prong monte−carlo

3−prong monte−carlo

data

Fig. 6

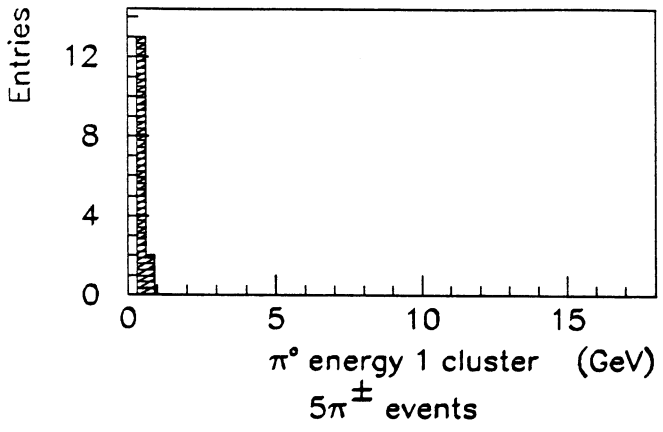
Entries
12
8
4
0
0
5
10
15
π° energy 1 cluster (GeV)
5π± events

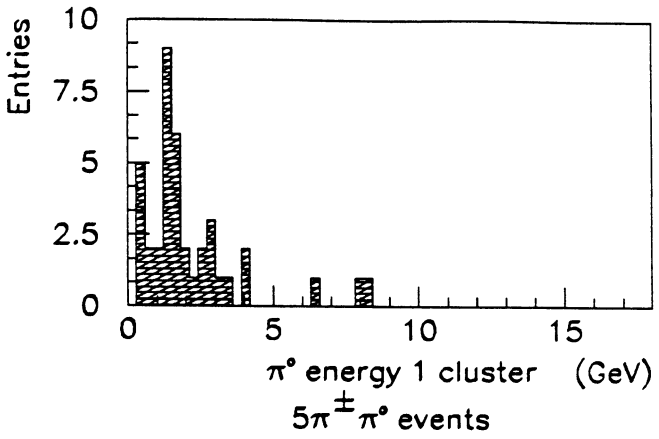
Entries
10
7.5
5
2.5
0
0
5
10
15
π° energy 1 cluster (GeV)
5π±π° events

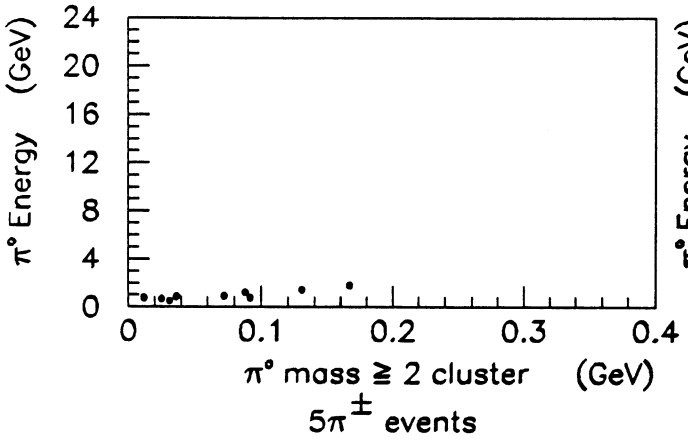
π° Energy (GeV)
24
20
16
12
8
4
0
0
0.1
0.2
0.3
0.4
π° mass ≧ 2 cluster (GeV)
5π± events

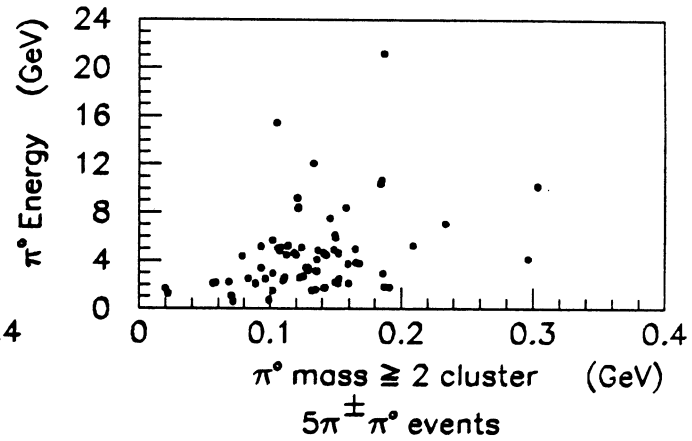
π° Energy (GeV)
24
20
16
12
8
4
0
0
0.1
0.2
0.3
0.4
π° mass ≧ 2 cluster (GeV)
5π±π° events

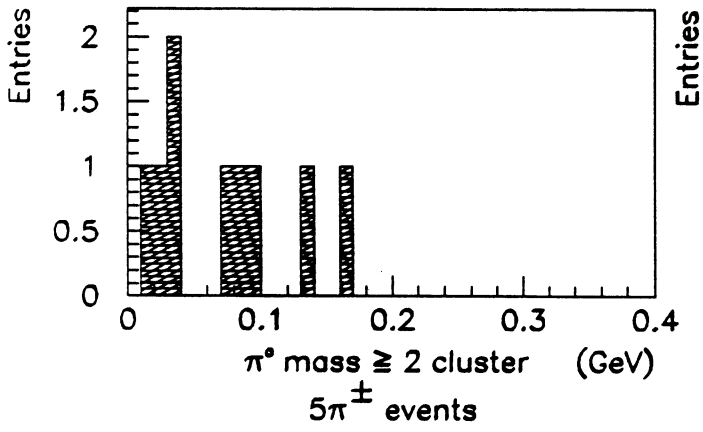
Entries
2
1.5
1
0.5
0
0
0.1
0.2
0.3
0.4
π° mass ≧ 2 cluster (GeV)
5π± events

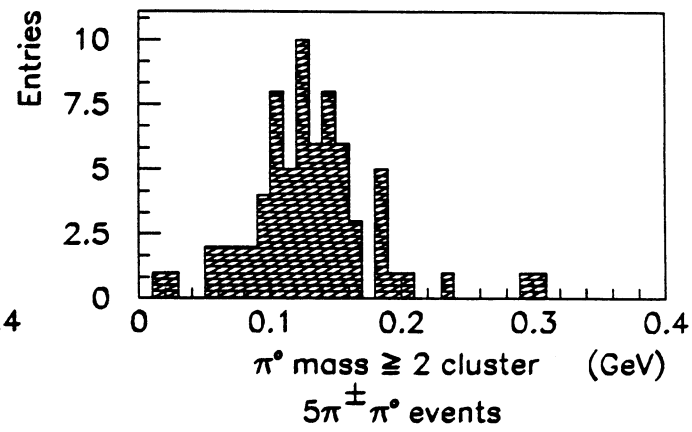
Entries
10
7.5
5
2.5
0
0
0.1
0.2
0.3
0.4
π° mass ≧ 2 cluster (GeV)
5π±π° events

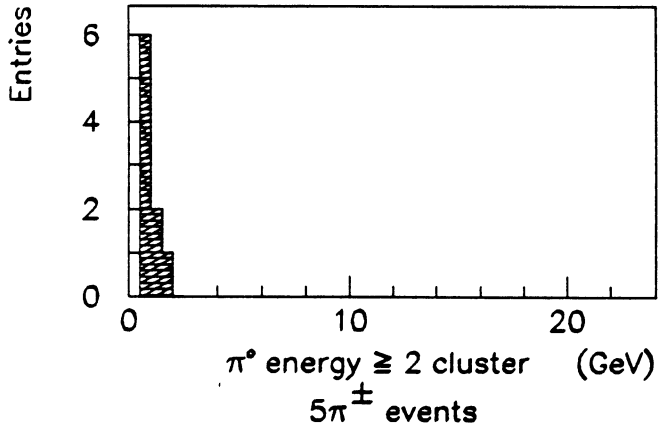
Entries
6
4
2
0
0
10
20
π° energy ≧ 2 cluster (GeV)
5π± events

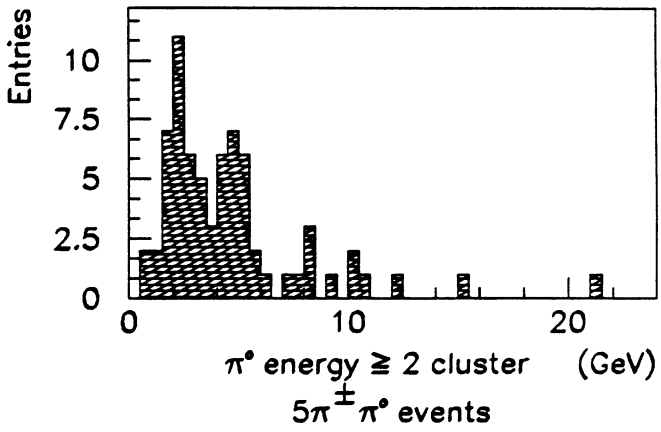
Entries
10
7.5
5
2.5
0
0
10
20
π° energy ≧ 2 cluster (GeV)
5π±π° events

Fig. 7

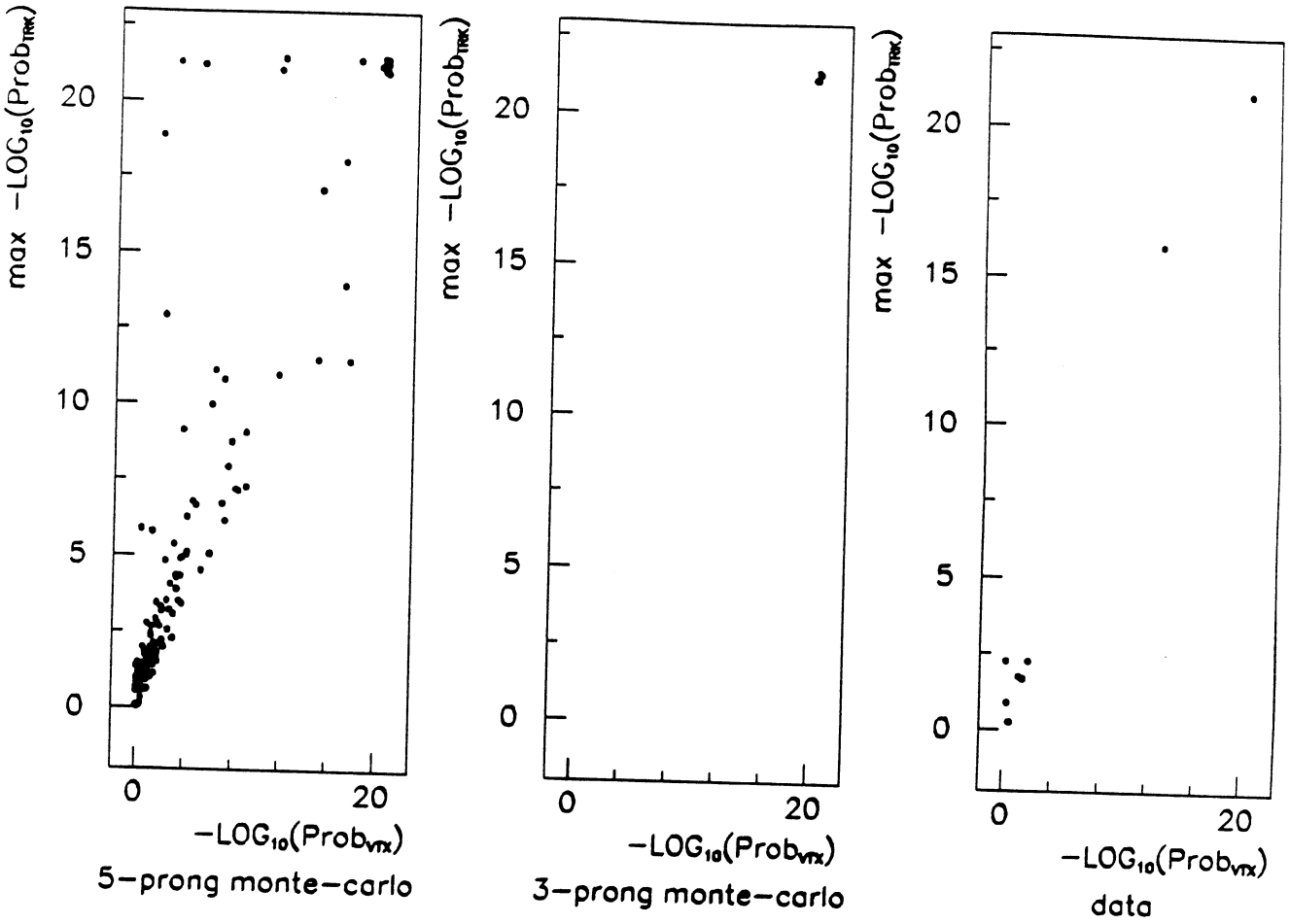
max −LOG10(ProbTRK)
−LOG10(ProbVTX)
5−prong monte−carlo
3−prong monte−carlo
data

Fig. 8

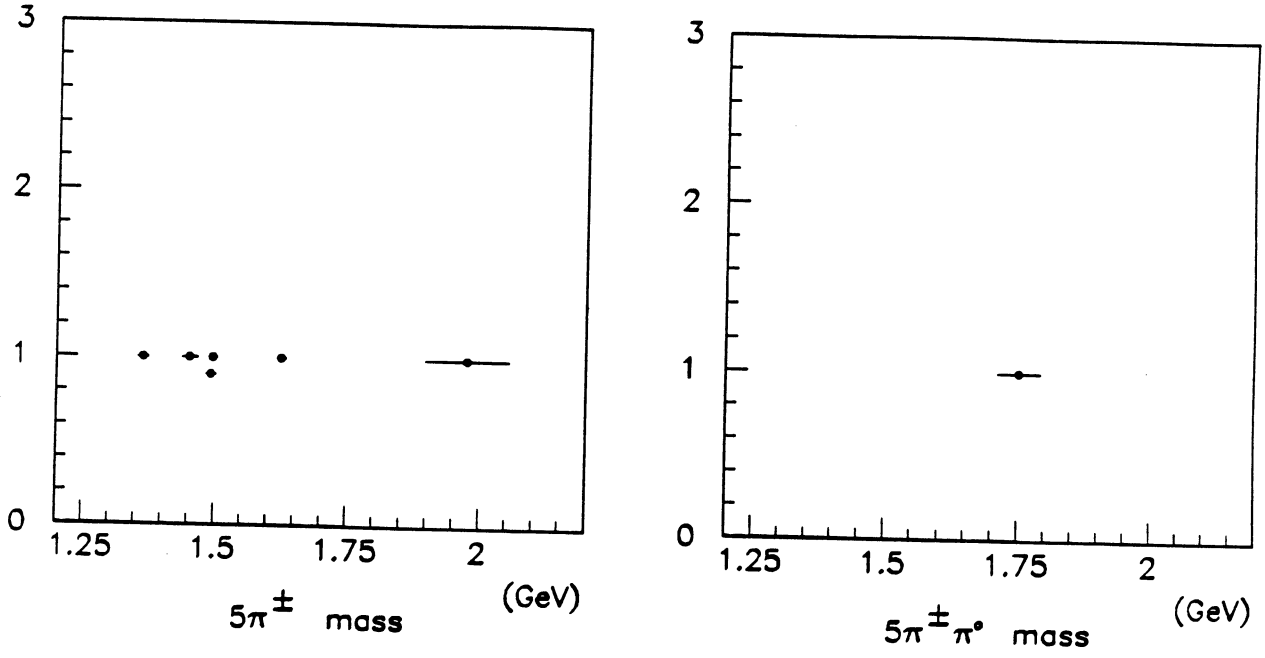
5π± mass
(GeV)
5π±π° mass
(GeV)

Fig. 9

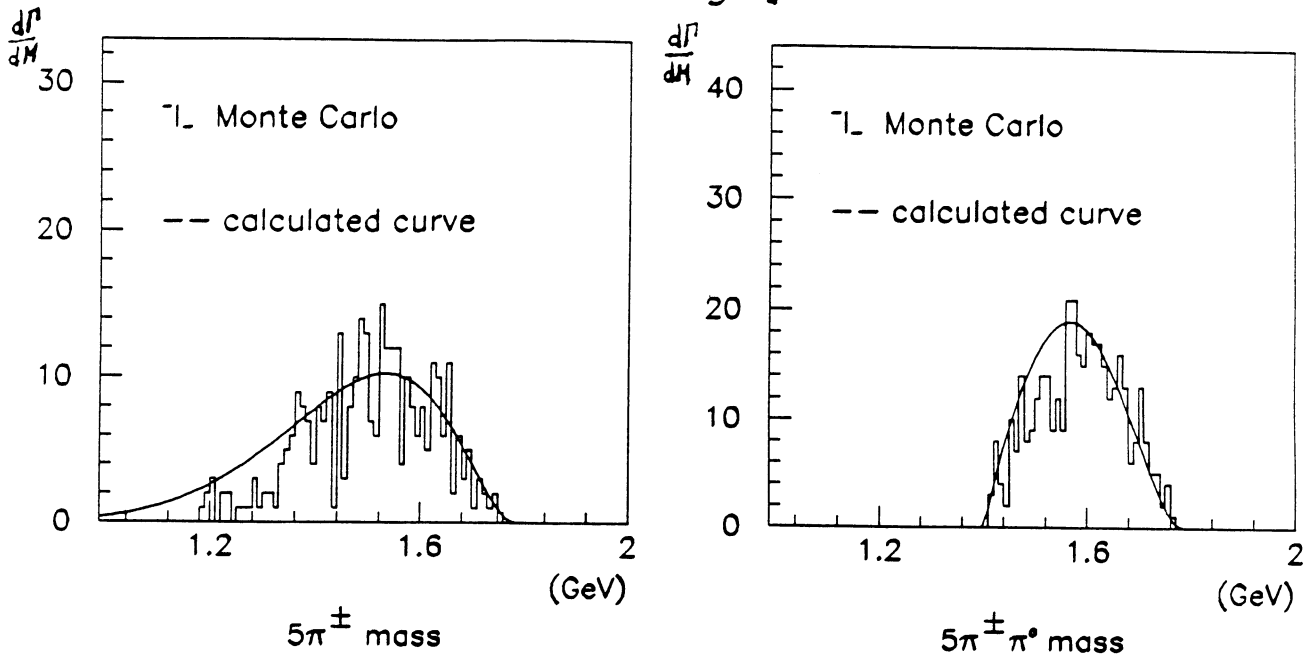
dN/dP
30
20
10
0
Monte Carlo
calculated curve
1.2
1.6
2
(GeV)
5π± mass
dN/dP
40
30
20
10
0
Monte Carlo
calculated curve
1.2
1.6
2
(GeV)
5π±π° mass

Fig. 10

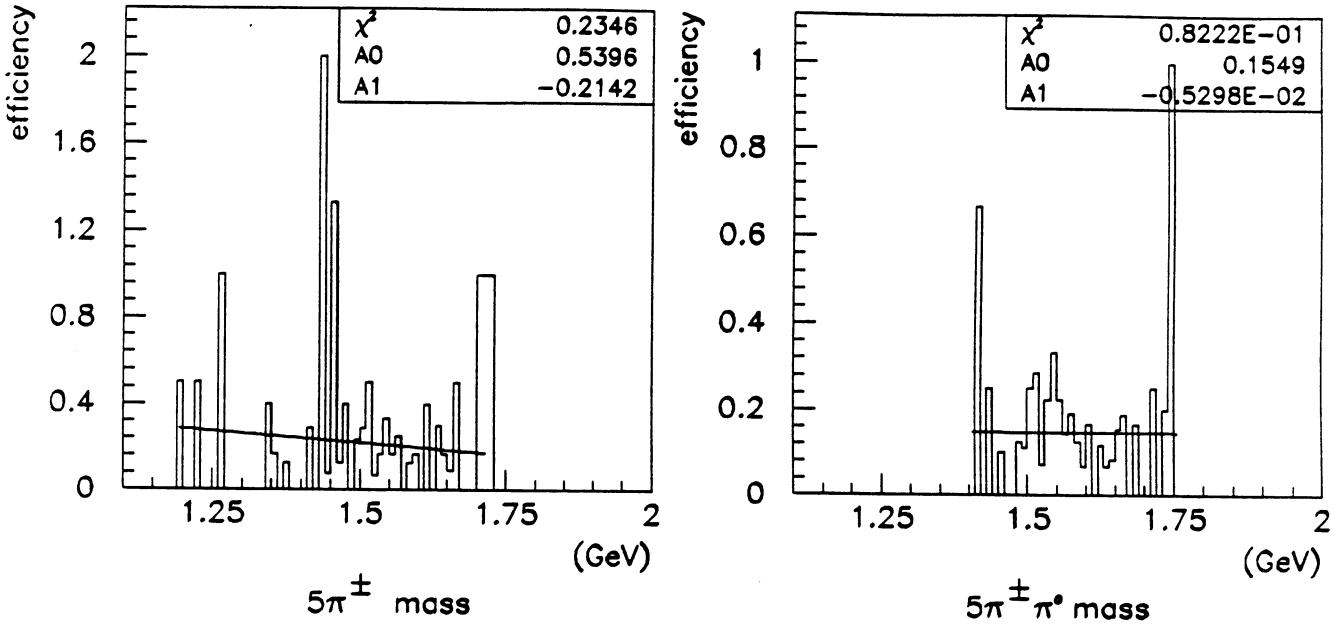
efficiency
2
1.6
1.2
0.8
0.4
0
χ² 0.2346
A0 0.5396
A1 −0.2142
1.25
1.5
1.75
2
(GeV)
5π± mass
efficiency
1
0.8
0.6
0.4
0.2
0
χ² 0.8222E−01
A0 0.1549
A1 −0.5298E−02
1.25
1.5
1.75
2
(GeV)
5π±π° mass

Fig. 11

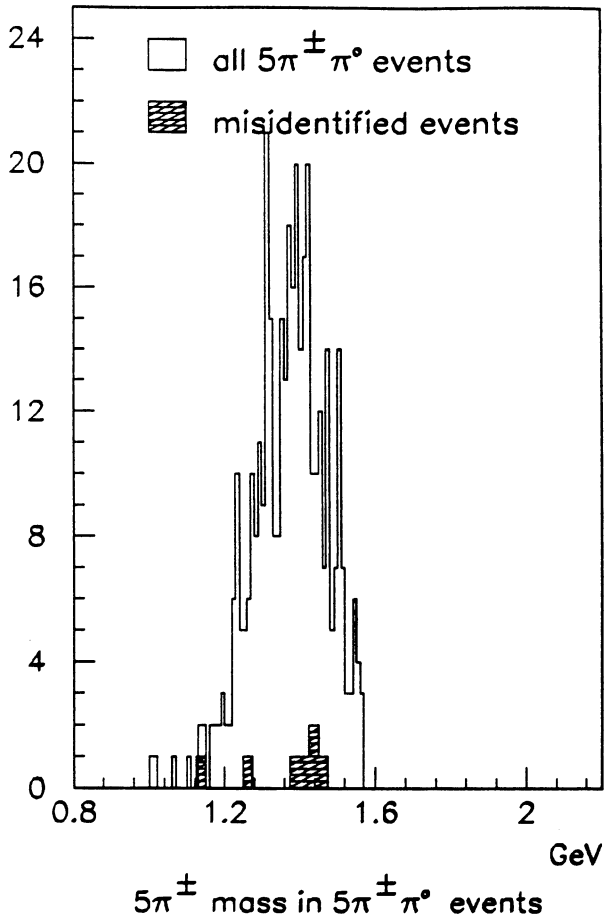
24
20
16
12
8
4
0
0.8
1.2
1.6
2
GeV
all $5\pi^{\pm}\pi^{\circ}$ events
misidentified events
$5\pi^{\pm}$ mass in $5\pi^{\pm}\pi^{\circ}$ events

Fig. 12

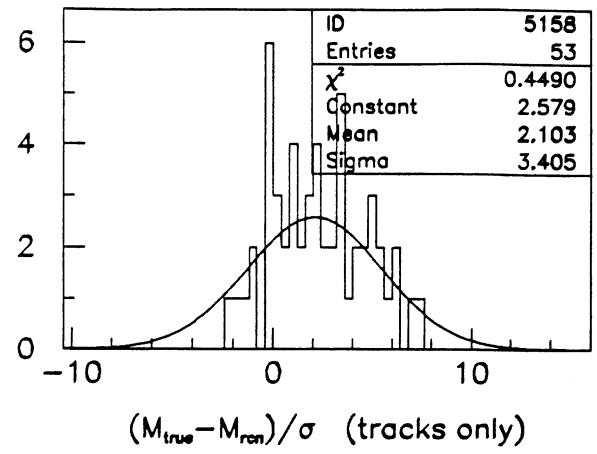
ID 5158
Entries 53
χ² 0.4490
Constant 2.579
Mean 2.103
Sigma 3.405
(M_true−M_rcn)/σ (tracks only)

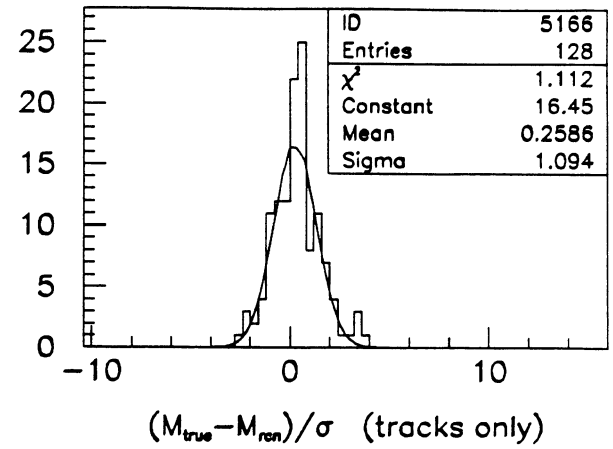
ID 5166
Entries 128
χ² 1.112
Constant 16.45
Mean 0.2586
Sigma 1.094
(M_true−M_rcn)/σ (tracks only)

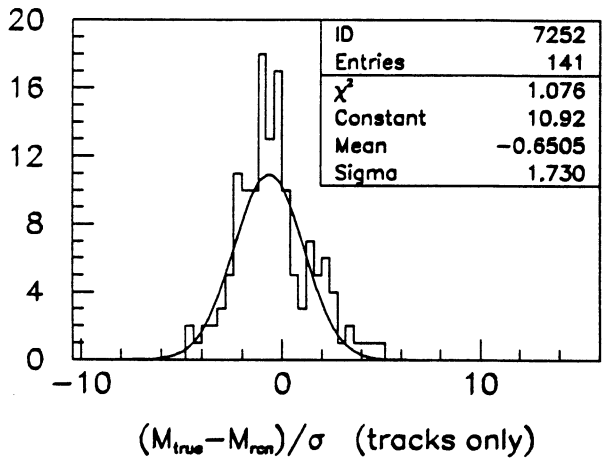
ID 7252
Entries 141
χ² 1.076
Constant 10.92
Mean −0.6505
Sigma 1.730
(M_true−M_rcn)/σ (tracks only)

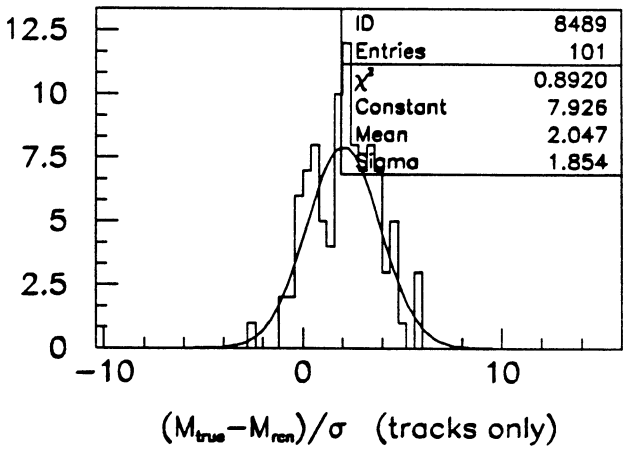
ID 8489
Entries 101
χ² 0.8920
Constant 7.926
Mean 2.047
Sigma 1.854
(M_true−M_rcn)/σ (tracks only)

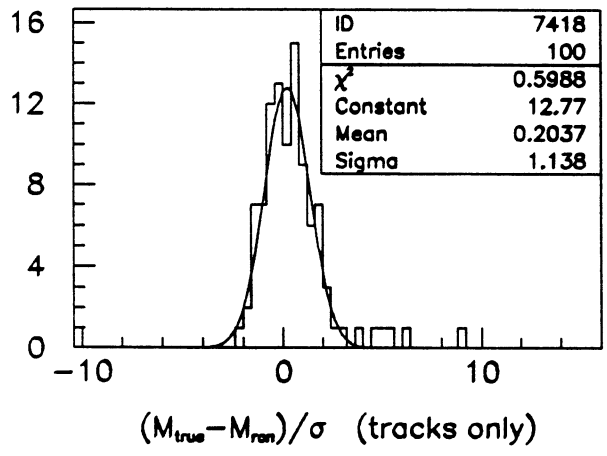
ID 7418
Entries 100
χ² 0.5988
Constant 12.77
Mean 0.2037
Sigma 1.138
(M_true−M_rcn)/σ (tracks only)

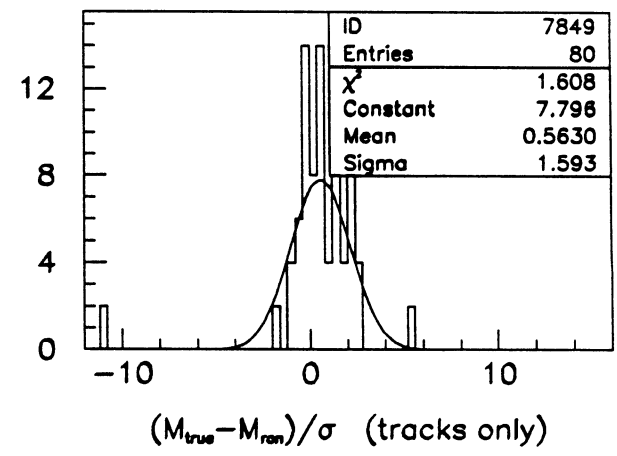
ID 7849
Entries 80
χ² 1.608
Constant 7.796
Mean 0.5630
Sigma 1.593
(M_true−M_rcn)/σ (tracks only)

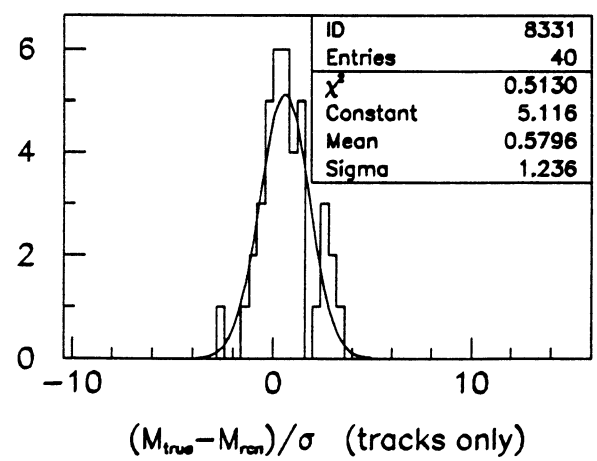
ID 8331
Entries 40
χ² 0.5130
Constant 5.116
Mean 0.5796
Sigma 1.236
(M_true−M_rcn)/σ (tracks only)

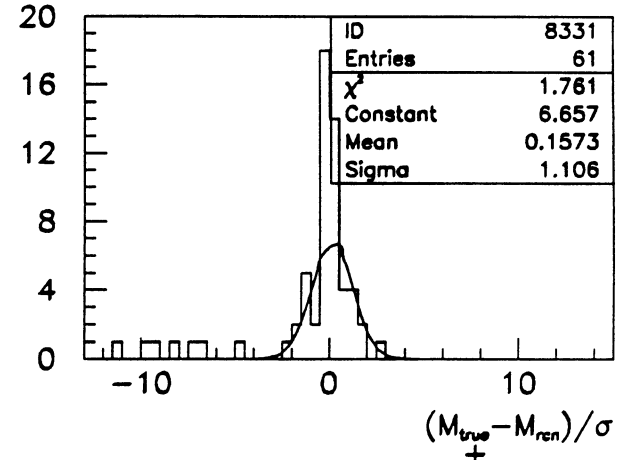
ID 8331
Entries 61
χ² 1.761
Constant 6.657
Mean 0.1573
Sigma 1.106
(M_true−M_rcn)/σ
resolution for all 5π±π°

Fig. 13

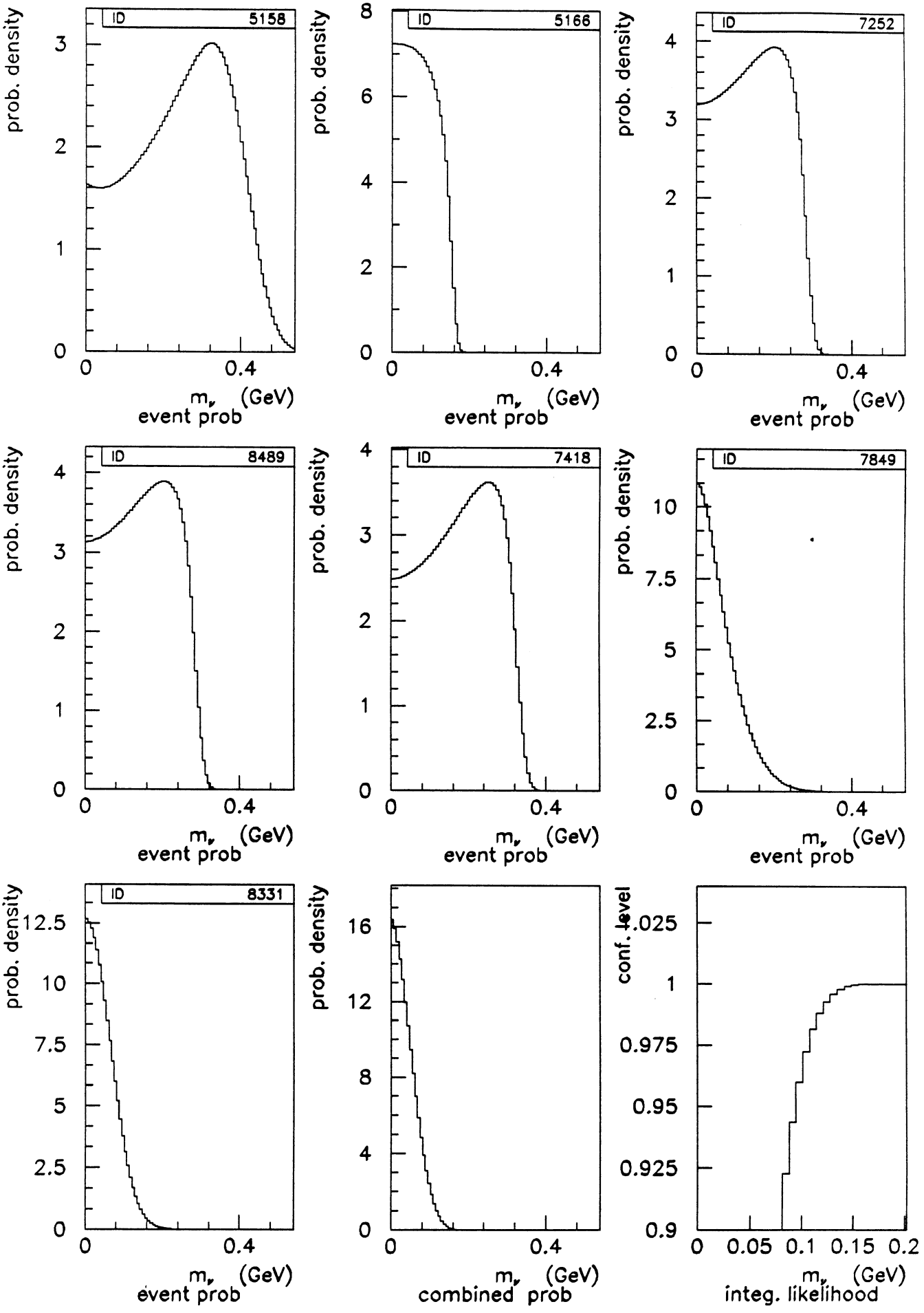
ID 5158
prob. density
m_{ν_τ} (GeV)
event prob
ID 5166
prob. density
m_{ν_τ} (GeV)
event prob
ID 7252
prob. density
m_{ν_τ} (GeV)
event prob
ID 8489
prob. density
m_{ν_τ} (GeV)
event prob
ID 7418
prob. density
m_{ν_τ} (GeV)
event prob
ID 7849
prob. density
m_{ν_τ} (GeV)
event prob
ID 8331
prob. density
m_{ν_τ} (GeV)
event prob
prob. density
m_{ν_τ} (GeV)
combined prob
conf. level
m_{ν_τ} (GeV)
integ. likelihood

Fig. 14